



Geopolymer Composite Coatings Based on Moroccan Clay and Sands for Restoration Application

Anass El Khomsi^{1,2}, Ameni Gharzouni¹, Remi Farges¹, Patrice Duport¹,
Nourredine Idrissi Kandri², A. Zerouale² and Sylvie Rossignol^{1*}

¹ IRCER: Institut de Recherche sur les Céramiques (UMR7315), Limoges, France, ² Laboratoire Signaux Systèmes & Composants, Faculté des Sciences et Techniques, Université Sidi Mohamed Ben Abdellah –Fès, Fes, Morocco

OPEN ACCESS

Edited by:

Dong-Kyun Seo,
Arizona State University, United States

Reviewed by:

Haitao Wang,
Nankai University, China
Jadambaa Temuujin,
Mongolian Academy of Sciences
(MAS), Mongolia

*Correspondence:

Sylvie Rossignol
sylvie.rossignol@unilim.fr

Specialty section:

This article was submitted to
Environmental Chemical Engineering,
a section of the journal
Frontiers in Chemical Engineering

Received: 15 February 2021

Accepted: 09 April 2021

Published: 31 May 2021

Citation:

El Khomsi A, Gharzouni A, Farges R,
Duport P, Idrissi Kandri N, Zerouale A
and Rossignol S (2021) Geopolymer
Composite Coatings Based on
Moroccan Clay and Sands for
Restoration Application.
Front. Chem. Eng. 3:667982.
doi: 10.3389/fceng.2021.667982

This study aims to explore geopolymer binders and mortars based on local Moroccan clays and sands as coatings for the restoration of historical monuments in Morocco. For this, five substrates, one geopolymer binder, and two geopolymer mortars were investigated. The characterization of substrates reveals differences in terms of pH value, capillarity, contact angle, and surface roughness. These differences affect the coating thickness, which also depends on the viscosity, liquid to solid ratio, and granular skeleton of the geopolymer coating. High adhesive strength values (up to 9 MPa) were obtained on limestones. However, these values decreased with the increase of relative humidity. In the case of Fez stone, a stable adhesive strength value (3 MPa) was evidenced for all the coating formulations and at different storage conditions confirming the suitability of coating based on metakaolin, Moroccan clays, and sands for restoration applications.

Keywords: coatings, mortar, binder, geopolymer, Moroccan clays

INTRODUCTION

Since antiquity, the construction of buildings was carried out using mortars and coatings based on air or hydraulic lime, historical monuments testify to the techniques and materials used. Often repair work is carried out with lime-based mortars and coatings, regardless of the place or time these monuments were built (Bozkurt and Yilmaz Demirkale, 2020). The nature of the substrates used depends very closely on the nature of the rocks and soil surrounding the construction sites (Loureiro et al., 2020). An example of this are the monuments of Sarno in Italy, where volcanic rocks characteristic of the region are found in the walls of different structures (Piovesan et al., 2019; Secco et al., 2019). With respect to the authenticity of these monuments, the mortars and plasters chosen for their restoration have been elaborated from raw materials similar to the original ones.

Restoration mortars and coatings must ensure a durable repair over time, and must resist weathering and natural hazards such as earthquakes, while keeping the authenticity of the monuments intact (Moropoulou et al., 1998, 2006). In order to fulfill all these functions, compliance with certain criteria for chemical, physical, and visual compatibility are required (Moropoulou et al., 2005; Ventola et al., 2011). As an example, in cement coatings, species penetrate by capillarity into the pores of masonry stones, and crystallize causing intrinsic stresses leading to irreversible damage (Benharbit, 2017). Concerning visual aspects, the external appearance of the monuments, including the color and texture of the materials, must preserve the symbolic character of the old constructions (ICOMOS, 2004; Schueremans et al., 2011). In most cases, the results are closer to the original

colors when local raw materials are used such as stones and clays. Another binder from a mixture of dolomite flour and clay underlines the effect of mineralogical composition (Kirilovica et al., 2018). Consequently, the physicochemical data of the raw materials are indispensable for the formulation of compatible materials, and their use should be preferred to meet the compatibility criteria.

In the last years, the use of geopolymers for cultural heritage restoration has garnered interest, and some works have been realized in that field. Occhipinti et al. (2020) showed that geopolymers made of 70–80% of pumice and 20–30% of metakaolin fulfill the criteria of chemical and mechanical compatibility with historical monuments. Hanzliček et al. (2009) worked on the restoration of a terracotta Baroque statue notably by repairing broken parts with a geopolymer mortar. The elaboration of a geopolymer restoration mortar for natural stones led to good results after a reduction in the quantity of activation solution and an increase in the extraction rate of aluminum thanks to the grinding process (Rescic et al., 2011), this could also reduce the formation of carbonate salts which is beneficial for restoration.

The adhesion between the support and the mortar is a crucial parameter. To evaluate this feature, several techniques were investigated. The effect of the curing temperature (40, 80, and 150°C) of the geopolymer coating on aluminum plates was tested using the scratch test (Mao et al., 2020). The best result was reached at a temperature of 40°C, without the formation of cracks or delamination. Deshmukh et al. (2017) studied the impact of the sodium meta-silicate/NaOH ratio and evidenced an amelioration of adhesion by a higher concentration of the activation solution (Skvara et al., 2006). Some authors investigated the relation between the roughness of the substrate surface and the adhesion, Nogami et al. (2015) showed that the adhesion of cement mortars is proportional to the surface roughness due to van der Waals forces. It has also been evidenced that in surfaces with lower relative humidity values, the adhesion forces are controlled by van der Waals forces, and at higher relative humidity values the capillary forces are predominant (Moutinho et al., 2017).

The aim of this paper is the elaboration of an airbrush-applied geopolymer coating for restoration works in Morocco. To achieve this objective, five geopolymer formulations were tested, the first three were binders based on metakaolin, and the two others were mortars based on Moroccan clays, limestone sand, and metakaolin. The five substrates (white and blue limestone, natural stones from Fez concrete, and plaster) selected were characterized before coating. The interaction between support and coating were evaluated by pull-off tests and a concentration profile (EDX-SEM).

MATERIALS AND METHODS

Raw Materials

The aluminosilicate precursors used were a commercial metakaolin (called M1) supplied by Argical, and two Moroccan clays A3 and A5 were calcined at 700°C (El Khomsi et al., 2020). For the mineral additives, two Moroccan limestone sands were

used, the first one called Sb1, mainly composed of calcite with some traces of quartz, and the second one Sb2, composed of dolomite and some traces of calcite. The sample preparation was carried out by mixing the aluminosilicate sources with a potassium silicate solution ($Si/K = 0.58$) (El Khomsi et al., 2020). Five substrates were used, blue and white limestone from a building material supplier, a sample of stone taken from a city near the Merinde tombs, and concrete and plaster from a building material supplier¹.

Coating Process

The coating deposition was carried out with an airbrush supplied by WilTec, using a nozzle diameter of 4.6 mm, an air pressure of 3 bars, an application distance between the airbrush and the substrate of 40 cm, and an interval of 10 min between the first and second layer of coating. The coated samples were left for 72 h in the laboratory for consolidation, then placed in three different storing atmospheres, laboratory conditions ($T = 20^\circ\text{C}$, $RH = 50\%$), high humidity ($T = 20^\circ\text{C}$, $RH = 85\%$), and outside conditions ($-2.3 \leq T \leq 19.4^\circ\text{C}$ and $40 \leq RH \leq 99\%$).

Sample Characterization

The viscosity measurements were performed with a Brookfield DV-II viscometer, 60 cm³ cylindrical pots were filled with reactive geopolymer mixture, and measurements were done every 30 min until the consolidation. The sealed pots were continually stirred on a lab roller at 60 rpm in laboratory conditions ($T = 20^\circ\text{C}$). The measured viscosity values were the average over a 1-min measurement, and the spindle's speed was set from 0.1 to 100 rpm, depending on the viscosity evolution. When viscosity reached the maximum measurable value (6,000 Pa.s), the measurements were stopped, indicating the consolidation of the material (Dupuy et al., 2020).

The wetting angles of the solid substrates were determined using the Digidrop MCAT apparatus from GBX. A drop of deionized water was deposited on the substrate, then the wetting angles were measured from the picture where the drop touched the substrate surface, using GBX's Visiodrop software. Wetting angle was measured five times with an estimated error of 4%.

The lightness measurements were operated using a Konica Minolta CM-600d spectro-colorimeter, the analyzed surface area was illuminated under a white light equivalent to natural day light. The lightness value (L^*) given by the apparatus was the average of three measurements on the same zone, and the measurements were made three times on every sample.

The pH meter used was a WTW 3310 equipped with a specific sensor for extreme pH values (calibrated in the range from 10 to 13). The pH values of the fresh reactive mixtures and consolidated samples were measured in water with a solid/liquid ratio of 0.08 and 0.1, respectively.

The roughness measurement was carried out using the HANDYSURF E-35A apparatus from ACCRETCH. The measurements were done ten times for each sample and every

¹ U. C. du patrimoine mondial, «Médina de Fès», UNESCO Centre du Patrimoine Mondial. Available online at: <https://whc.unesco.org/fr/list/170/>.

measured value R_a was the average roughness of a fifth of a section.

The adhesive strength of the coated samples was evaluated by a pull-off test using an Elcometer 510 adhesion tester, according to ASTM D4541. Every measured value was an average of at least two measurements with a standard deviation of ± 0.5 MPa. A 20 mm model was stuck to the coating using epoxy glue, and the test was carried out after 24 h of glue consolidation.

A freeze-thaw cycle was completed in a climatic chamber (ClimEvent C/180/70/3), each cycle had a duration of 5 h including a phase at 20°C and 95% RH and another phase at -20°C and 0% RH.

X-ray diffraction (XRD) was carried out with a Bruker-D8 Advance with Bragg-Brentano geometry equipped with a Cu $K\alpha 2$ detector. The analytical range is between 5 and 55° (2 θ) with a resolution of 0.02° and a dwell of 1.5 s. The phase was

identified with reference to a powder diffraction standard of the joint committee (JCPDS).

Microstructural observations were made with a JEOL IT 300 LV scanning electron microscope at 10 kV, equipped with a tungsten source, and an X chemical. The samples were metalized by the deposition of a 10 nm layer of Pt or carbon, and then stuck to the metallic support using silver lac to facilitate electronic conduction.

RESULTS

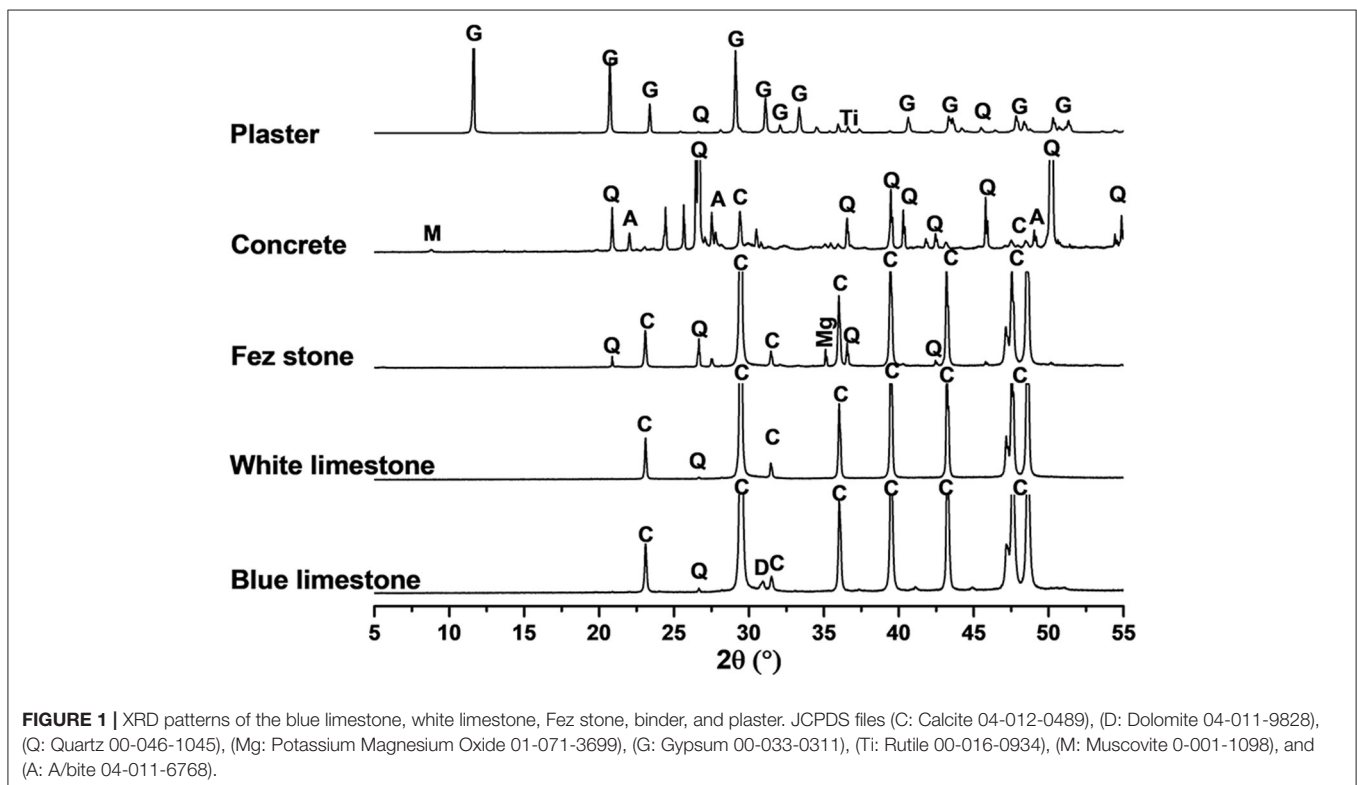
Substrates Characteristics and Selection of Binder/Mortars Formulations

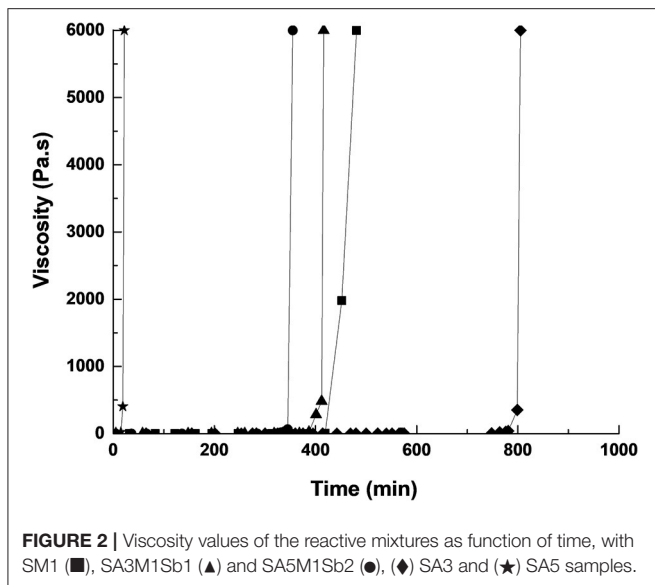
The understanding of both the substrates and the binders or mortars characteristics was necessary to realize the coating.

Table 1 summarizes the physicochemical characteristics of the five supports. According to the data, two categories of materials can be distinguished; the first one was represented by the natural stones (white and blue limestone as well as Fez stone) with pH values around nine, which is in accordance with calcite-based substrates found in literature (Benjeddou et al., 2017). The second category was characterized by an alkalinity around 11 for concrete (10.3) and plaster (11.5). These two categories were also distinguished by their capillarity values, for the natural stones, a low capillarity was observed varying from 0.2 to 5 ($\text{g}/\text{m}^2 \cdot \text{s}^{0.5}$), and for concrete a higher value of 11.8 ($\text{g}/\text{m}^2 \cdot \text{s}^{0.5}$) was measured. The porosity of these materials were in accordance with their capillarity, indeed, natural stones had a low percentage of open porosity, varying from 0.3 to 5.1%, whereas a higher value was

TABLE 1 | Values of pH, capillarity, porosity, contact angle, and roughness of the used supports.

Support	pH value ± 0.1	Capillarity ($\text{g}/\text{m}^2 \cdot \text{s}^{0.5}$)	Porosity (%) ± 0.1	θ_{water} (°) ± 3	R_a (μm) ± 0.1
White limestone	9.2	4.7	4.2	67	2.7
Blue limestone	8.9	0.2	0.3	91	1.3
Fez stone	8.9	1.6	5.1	85	3.5
Concrete	10.3	11.8	13.6	41	7
Plaster	11.5	51.8	54.0	41	1.0





observed for concrete (13.6%). Some authors reported similar porosity values for limestone, varying from 0.27 to 4.1%, which corroborates the measured values (Waples and Waples, 2004; El Alami et al., 2020). The contact angles of water with the different supports showed two kinds of behaviors, the natural stones exhibited contact angles of 67, 91, and 85° for the white, the blue limestone, and Fez stone, respectively. The second category, represented by concrete and plaster showed an identical contact angle of 41°, which indicated that the second category was more hydrophilic than natural stones. Concerning the roughness of the different substrates, the values were 2.7, 1.3, and 3.5 μm for the white, the blue limestone, and Fez stone, respectively, whereas for concrete and plaster the values were 8.5 and 1 μm , respectively. These values were in accordance with the observed contact angles, indeed, the increase of roughness led to higher hydrophilicity, which was observed and is in accordance with literature, some authors reported that the increase of limestone roughness led to lower contact angles with water (Sharma et al., 2018). All these data underline the fact that both porosity and capillarity vary in opposite to wetting angle. These differences in the physicochemical properties could have an impact on the physical interactions between the coating and the substrate, especially in terms of the anchoring and penetration of the fresh coating mixtures.

The X-ray patterns are gathered in **Figure 1**. All the substrates displayed the presence of the crystalline phase corresponding to their chemical content. For blue and white limestone, the main mineral was calcite, with some traces of dolomite and quartz. For the Fez stone, it was similar with some magnesium oxide. For the concrete, there was quartz, calcite, dolomite, albite, and muscovite. Finally, the plaster sample contained gypsum, with some impurities in trace quantities like quartz and titanium dioxide. There was clearly three types of materials from the mineralogical point of view, which could lead to a different chemical interaction between the coatings and the substrates.

TABLE 2 | Weight loss resistance to compression and density of the selected binders and lightness.

Selected binders	Weight loss (30–250°C)	σ (MPa)	ρ (g/cm ³)	L* (%)
SM1	30	34	1.57	82
SA3M1Sb1	24	33	1.87	53
SA5M1Sb2	28	21	1.79	54

In order to select the optimal formulations of the coating, five geopolymer mixtures were studied: three binders based on metakaolin or Moroccan clays (S1M1, S1A3, and S1A5), and two mortars based on mixtures of metakaolin, Moroccan clays, and aggregates (S1A5M1Sb2 and S1A3M1Sb). The use of local clays ensures a chemical compatibility with the monuments and is strongly advised in literature (Apostolopoulou et al., 2018; Loureiro et al., 2020), because the mineralogical composition of the surrounding materials are usually similar to those of monuments, due to the common geographical location (Apostolopoulou et al., 2018; Loureiro et al., 2020). Additionally, the presence of associated minerals act as fillers and prevent the appearance of cracks on the coating. It is also a way to valorize these materials and reduce the cost of the coating because these clays are abundant. The difference between the Moroccan clays and the metakaolin in terms of mineralogical composition is the presence of an associated mineral such as quartz, calcite, dolomite, and muscovite. The viscosity evolution as a function of time of the five geopolymer reactive mixtures was investigated (**Figure 2**). Whatever the sample, all curves showed a first part where the viscosity was quite low and stable then a sharp rise of viscosity was noticed, indicating the consolidation of the materials following the polycondensation reaction. The setting time can then be measured by the tangent method (Arnoult et al., 2018). Different consolidation times can be observed for the various formulations. The curve of SA3 formulation showed an initial viscosity value around 0.1 Pa.s up to 370 min, after that, the viscosity increased. The consolidation time corresponded to 13 h, which was too long for the targeted application. For the SA5 formulation the mixture consolidated in 5 min, which was too short for spray projection, consequently these two formulations were eliminated. Concerning, the three formulations SM1, SA3M1Sb1, and SA5M1Sb2, the setting time was around 400 min and was favorable for spray projection. Consequently, these formulations were selected to be used as coating. **Table 2** gathers some data issued from previous works (El Khomsi et al., 2020). The binder SM1 presented a mechanical resistance of 34 MPa, a density of 1.57 g/cm³, and a water content of 30%. The second formulation SA3M1Sb1 was a mortar, it had similar mechanical strength, a higher density of 1.87 g/cm³, and less water content (24%) due to its higher solid content. The last formulation SA5M1Sb2 had the lowest mechanical strength (21 MPa) due to the low reactivity of the A5 clay which had a lower kaolinite content than A3 (El Khomsi et al., 2020), a density of 1.79 g/cm³, and a water content of 28%.

The five studied substrates showed two categories of physical and chemical characteristics. Furthermore, a binder and two

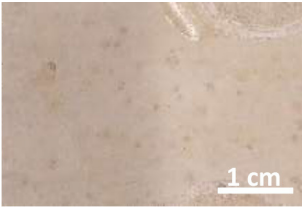
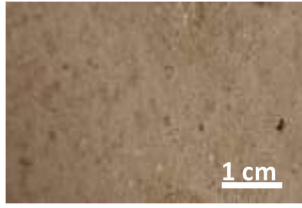
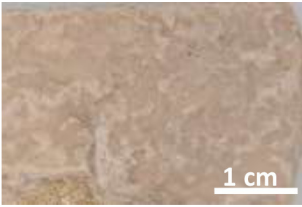
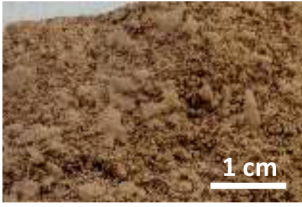
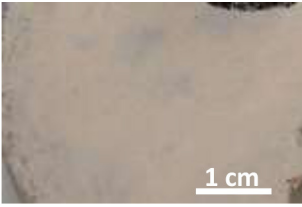
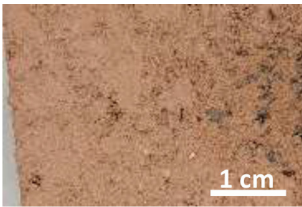
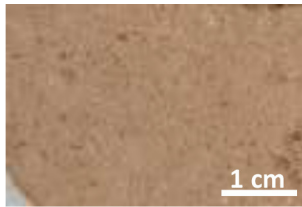
mortars were selected for the coating application, which suggest different interactions between the various coatings and substrates.

Binder and Mortars Coating

The application of coatings on the five substrates was feasible by the airbrush method, the viscosity of the freshly selected

mixtures SM1, SM1A3Sb1, and SM1A5Sb2 was not too high and the 4 mm noodle was sufficient to allow projection. It was also possible to apply two layers with an interval of 10 min due to the stable viscosity. **Table 3** shows the three coatings SM1, SM1A3Sb1, and SM1A5Sb2 applied on the white limestone, Fez stone, and concrete as well as their lightness. The SM1 coating had a thin aspect and a bright beige color (the highest lightness

TABLE 3 | Pictures and lightness of SM1, SM1A3Sb1, and SM1A5 Sb2 coatings applied on white limestone, Fez stone, and concrete.

Substrates	Coating formulation		
	SM1	SM1A3Sb1	SM1A5Sb2
White limestone	 <p>L (79%) * a (2%)*b (11%)</p>	 <p>L (61%) *a (11%) *b (18%)</p>	 <p>L (62%) *a (9%) *b (17%)</p>
Fez stone	 <p>83%</p>	 <p>60%</p>	 <p>62%</p>
Concrete	 <p>70%</p>	 <p>51%</p>	 <p>58%</p>

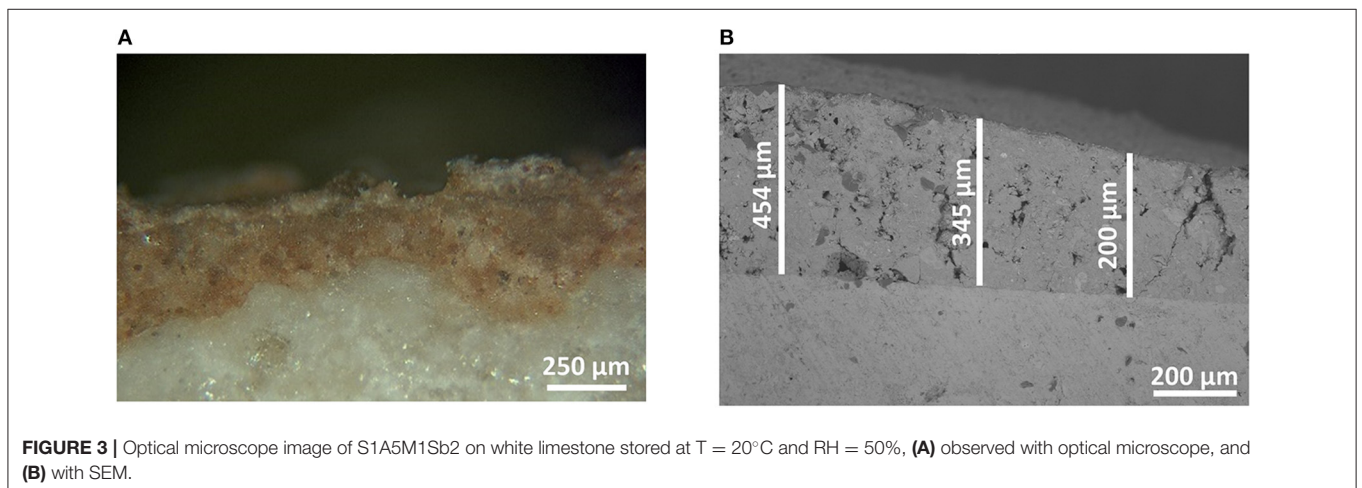
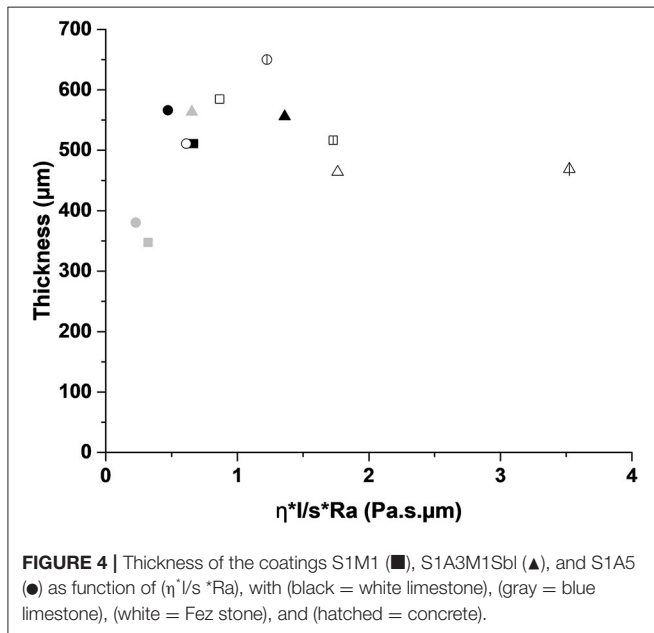


TABLE 4 | Thickness of the different coatings sprayed on the five substrates.

Substrates	Coating thickness		
	SM1 (μm)	SA3M1Sb1 (μm)	SA5M1Sb2 (μm)
White limestone	511	556	566
Blue limestone	348	564	380
Fez stone	585	464	511
Concrete	517	469	650
Plaster	430	433	500



of 79, 83, and 70% on white limestone, Fez stone, and concrete, respectively), the second coating SM1A3Sb1 was reddish with apparent aggregates, and for SM1A5Sb2 aggregates were also apparent but the color was less intense than SM1A3Sb1 which was in accordance with the measurement which showed a slightly lower lightness for SM1A3Sb1 compared to SM1A5Sb2. The color of SM1 was bright beige ($a = 2\%$ and $b = 11\%$), for SM1A3Sb1, parameter a^* was higher (11%) which indicated a more reddish color, and for the third coating SM1A5Sb2, the reddish tone was less accented ($a = 9\%$), with a more prominent yellow color ($b = 17\%$). These differences in color could be due to the presence of iron in the geopolymer matrix. As it can be observed, the variation of a^* and b^* were in agreement with the L -value. That is the reason why in this text, there are only the values of L . Moreover, the difference of colors in the presence of Moroccan clays was in relation to the iron presence. This means that this mixture depends on its environment to induce differences in color.

The coating thickness was determined from optical microscope and SEM observation. **Figure 3** shows an example of optical and SEM images for the SM1A5Sb2 mortar coating on white limestone. It can be seen that the coating displayed a continuous layer of thickness of $500 \mu\text{m}$ without any defect at the interface. Consequently, the thickness values of all the

samples are gathered in **Table 4**. For the white limestone, the thickness values were similar and relatively high regardless of the coating formulations (about 511 , 556 , and $566 \mu\text{m}$ for SM1, SM1A3Sb1, and SM1A5Sb2 formulations, respectively). On the blue limestone, the value decreased slightly (348 and $380 \mu\text{m}$ for SM1 and SM1A5Sb2 samples, respectively). For Fez stone, the thicknesses were similar to those observed for white limestone (varying from 464 to $585 \mu\text{m}$ for SM1A3Sb1 and SM1 coatings, respectively). For concrete, the thickness values were in the same range (517 , 469 , and $650 \mu\text{m}$ for SM1, SM1A3Sb1, and SM1A5Sb2 formulations, respectively). These values are in accordance with those obtained in literature (Temuujin et al., 2010). To understand the difference, the thickness of each coating was plotted in function of surface roughness corrected by the viscosity and the liquid to solid ratio ($Ra \cdot \eta^*I/s$) in **Figure 4** (Pierre, 1992; Gajanan Kunde and Ganapati Yadav, 2016). The observed variation underlines two types of behavior. First, a quasi-linear increase of the coating thickness from 340 until $650 \mu\text{m}$ with the increase of $(Ra \cdot \eta^*I/s)$ from 0.13 to 1.1 Pa.s . μm , then a slight decrease and a stabilization at about $460 \mu\text{m}$ for a value of $(Ra \cdot \eta^*I/s) > 1.1 \text{ Pa.s}$. μm . The binder SM1 led to a thin coating which increased in thickness with the increase of substrate surface roughness in this order (plaster < blue limestone < white limestone < Fez stone and then decreased slightly in the case of concrete. This fact can be explained by its low viscosity (0.19 Pa.s), high pH value (13.15) at the moment of the application, and the absence of aggregates. The decrease of thickness in the case of concrete was due to its heterogeneous surface. The mortar SM1A5Sb2 exhibited a similar trend due to its low initial viscosity (0.25 Pa.s) and high pH value (13.03). The presence of Sb2 sand with a larger particle size (the D_{50} was 9 and $46 \mu\text{m}$ for A5 and Sb2, respectively) favored the granular skeleton (El Khomsi et al., 2020). The mortar SM1A3Sb1 had different behavior with a relatively more stable value of thickness varying between 450 and $550 \mu\text{m}$ and less dependent on roughness of substrates. Its higher initial viscosity (0.95 Pa.s) can explain this fact and its lower initial pH value (12.96) compared to the other coatings revealed lower granular interactions. Furthermore, the used sand in this case exhibit a D_{50} similar to the clay A3 ($16 \mu\text{m}$) which did not favor the granular skeleton.

Thus, the coating thickness depends on the coating characteristics such as viscosity, liquid to solid ratio, and granular skeleton in the case of mortar as well as the substrate's surface roughness.

Adhesive Strength and Impact of Storage Conditions

In order to verify the adhesion and the stability of the different coatings and substrates, they were stored for 50 d in different conditions: laboratory conditions ($T = 20^\circ\text{C}$ and $\text{RH} = 50\%$), humid conditions ($T = 20^\circ\text{C}$ and $\text{RH} = 85\%$), and outside conditions ($-2.3 \leq T \leq 19.4^\circ\text{C}$ and $40 \leq \text{RH} \leq 99\%$). Pull-off tests were performed, and two types of failure were evidenced as shown in **Table 5**. For the two limestones and Fez stone, a cohesive failure was observed. That meant that the coating failed within the body of the coating leaving it on the surface of the substrate and on the dolly face. For concrete and plaster, a substrate failure was observed which meant that the bond

TABLE 5 | Picture of the adhesive and cohesive failures of the three coatings applied on the five substrates, stocked at 20°C, 50% HR, during the pull-off tests.

Support	S1M1	S1 A3M1Sb1	S1 A5M1Sb2
White limestone			
Blue limestone			
Fez stone			
Concrete			
Plaster			

between the coating and the substrate exceeded the strength of the substrate itself. In this case, concrete and plaster were removed from the surface and can be seen on the coating on the dolly face. **Figure 5** shows the obtained adhesive strengths at different conditions. In laboratory conditions ($T = 20^{\circ}\text{C}$ and $\text{RH} = 50\%$, **Figure 5A**), regardless of the coating formulation, the white and blue limestone exhibited the highest adhesive strength varying from 6 to 9 MPa. The Fez stone showed an adhesive strength in the range of 2.5–3.5 MPa, and concerning the concrete and plaster, the adhesive strength was lower than the previous substrates, around 2 MPa. The increase of humidity ($T = 20^{\circ}\text{C}$ and $\text{RH} = 85\%$, **Figure 5B**) led to a general decrease of the adherence in the outside conditions, and a more pronounced decrease of the adhesive strength was observed, especially for blue limestone (2.5–4 MPa). Consequently, all the coatings resisted the different storage conditions except the plaster substrate which showed coating detachment for all the formulations in real conditions. This fact can be explained by the highest porosity and capillarity in plaster (**Table 1**) compared to the other substrates

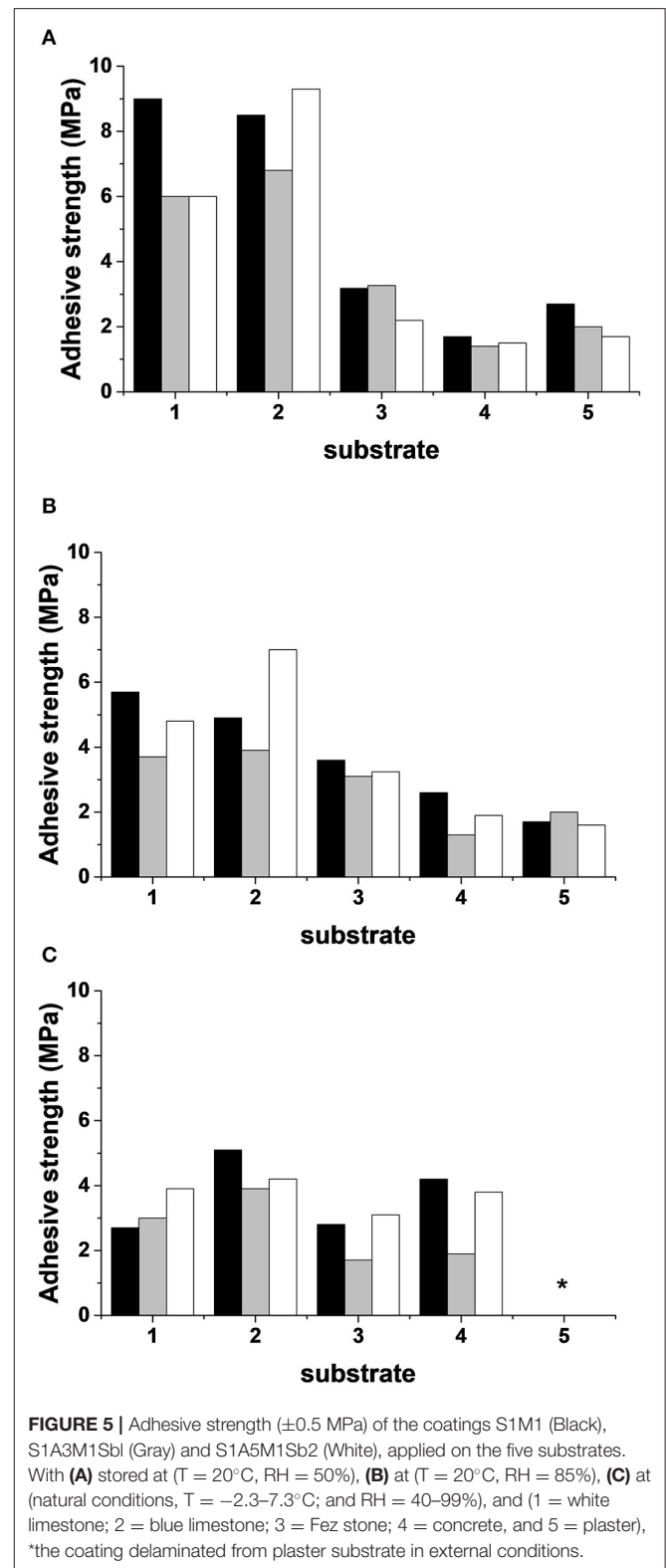
leading to high moisture retention weakening the bond with the geopolymer coating (Dalehaug, 2005). Furthermore, all the obtained adhesive strength values were superior to 1 MPa, which verified that the selected formulations were suitable for coating application (Jiang et al., 2020). All the samples were exposed to freeze-thaw cycles to check the formation of efflorescence. **Table 6** shows the pictures of the coatings after 20 freeze-thaw cycles and there was no white patches formation on the surface. This fact can be explained by the use of potassium silicate solution as an activator, which reduces the efflorescence formation because potassium is strongly bound (Duxson et al., 2006) to the aluminosilicate geopolymer network, limiting the leaching of that element and reducing the risk of efflorescence (Najafi Kani et al., 2012).

The adhesive strength values were plotted in function of the substrate surface roughness, except for plaster, at the different storage conditions in **Figure 6**. A general trend showing a decrease then a stabilization of the adhesive strength with the increase of the substrate surface roughness was noticed. At

ambient laboratory conditions ($T = 20^{\circ}\text{C}$ and $\text{RH} = 50\%$), SM1 exhibited the highest adhesive strength whatever the substrate compared to the other two mortars. The highest adhesive strength values were obtained for white, blue limestones, and Fez stone (9, 8.5, and 3.5 MPa, respectively) characterized by a low roughness (2.7, 1.3, and $3.5\ \mu\text{m}$) and high contact angle (67° , 91° , and 85° , respectively). The lowest adhesive strength values were obtained for concrete, which exhibited higher roughness and lower contact angle ($8.5\ \mu\text{m}$ and 41° , respectively). The two mortars showed similar results. It is well-known that adhesion increases with the increase of roughness surface (Mao et al., 2020). However, in this case, different substrates were compared. Their different physical and chemical structures induce different interactions due to different surface tensions and contact angles similar to the behavior of glasses (Sanjay Latthe et al., 2019). Indeed, the increase of roughness can lead to the creation of weak spots generating stress in the interface between the coating and the substrate (Chiche et al., 2000). At higher relative humidity ($T = 20^{\circ}\text{C}$ and $\text{RH} = 85\%$), a decrease of the adhesive strength was only observed in the case of the two limestones (6, 4, and 5 MPa for SM1, SM1A3Sb1, and SM1A5Sb2 coatings, respectively). For the other substrates, no changes were detected. This fact can be explained by the higher sensitivity of limestone to humidity weakening the bond between the substrate and the coating (Ciantia et al., 2014; Randazzo et al., 2020). Similar results were obtained for outside condition storage with a higher decrease of the adhesive strength in the case of limestone (about 3 and 4 MPa for the three coatings on white and blue limestones, respectively). However, no significant change was detected on Fez stone and concrete. Consequently, the substrate properties (surface roughness and sensitivity to humidity) seemed to control the adhesion between the geopolymer formulations and the different substrates. Quite stable adhesive strength values were obtained for Fez stone regardless of the coating formulation and the storage conditions.

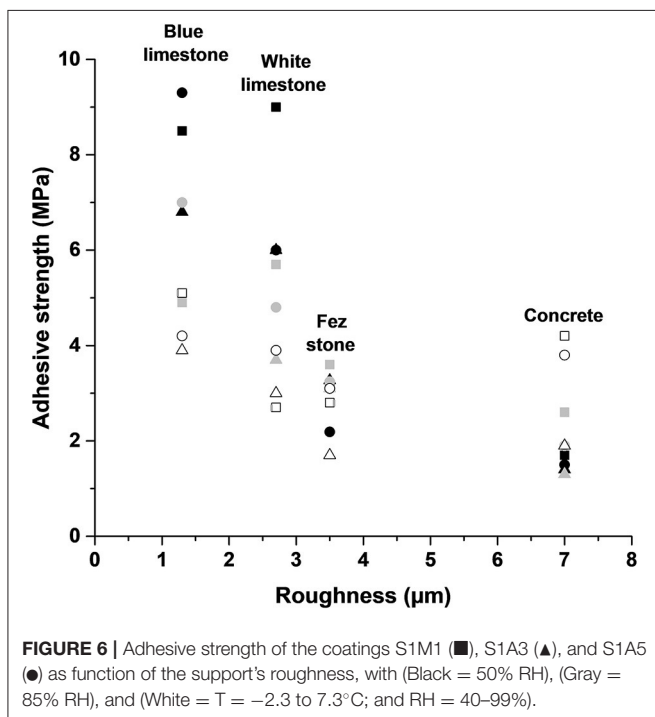
In order to determine the nature of the interfacial bonding between the studied coatings and substrates, SEM photos as well as a concentration profile of the major elements Si ($K\alpha = 1,739\ \text{keV}$), Al ($K\alpha = 1,486\ \text{keV}$), K ($K\alpha = 3,312\ \text{keV}$), and Ca ($K\alpha = 3,690\ \text{keV}$) were investigated. The elements Si and K were the main constituents of the geopolymer network, and Ca was the major component of limestone and concrete, therefore only concentration profiles of Si, K, and Ca elements were presented, as shown in Figure 7. The other photos are reported in the Supplementary Material. The geopolymer and the stone showed two distinct microstructures. For the SM1 binder (Figure 7A), the observed crack in the interface was due to the preparation of the sample. The coating layer SM1 showed the presence of Si and K which decreased drastically at the expense of the increase of calcium, a characteristic of Fez stone due its calcareous nature. The same results can be observed for the two mortars SA3M1Sb1 and SA5M1Sb2 (Figures 7B,C), respectively.

At this scale, it is difficult to detect the penetration of the coating in the substrate. For this, a zoom was done on the interface between the SM1A5Sb2 mortar and two substrates: Fez stone (Figure 8A) and concrete (Figure 8B). The concentration profiles of Si, K, Al, Mg, and Ca elements were plotted. A



progressive decrease of Si, Al, and K elements and an increase of Ca was observed in the interface denoting small penetration transition zones of about 4 and $8\ \mu\text{m}$ in the case of Fez stone and concrete, respectively showing the penetration. The larger

TABLE 6 | Picture of coated Fez stone before and after 20 freeze-thaw cycles.



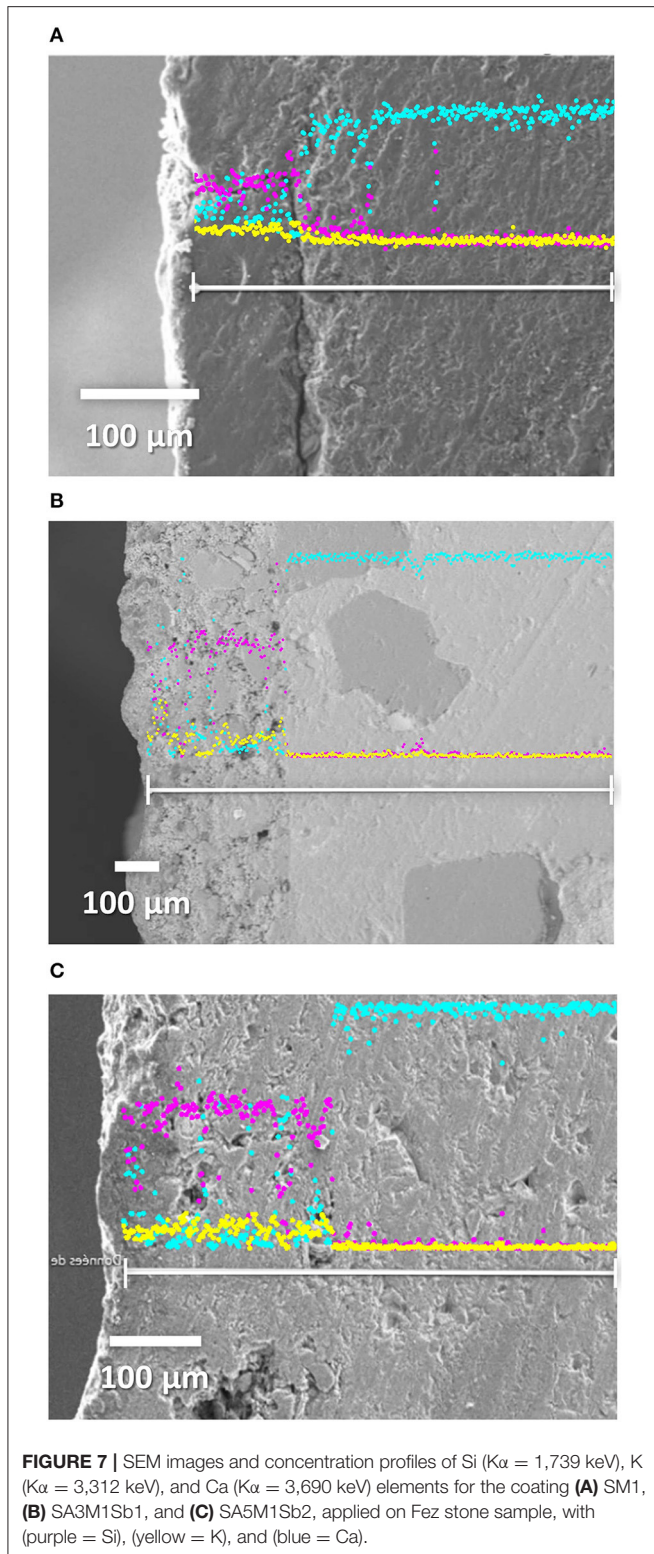
penetration zone in the case of concrete can be explained by higher affinity due to similar chemical composition with the geopolymer mortar and the higher porosity of concrete. This result is in accordance with literature (Zhang et al.,

2010; Pareek et al., 2018). Consequently, the adhesion of the geopolymer binder or mortars on the different substrates was not purely mechanical.

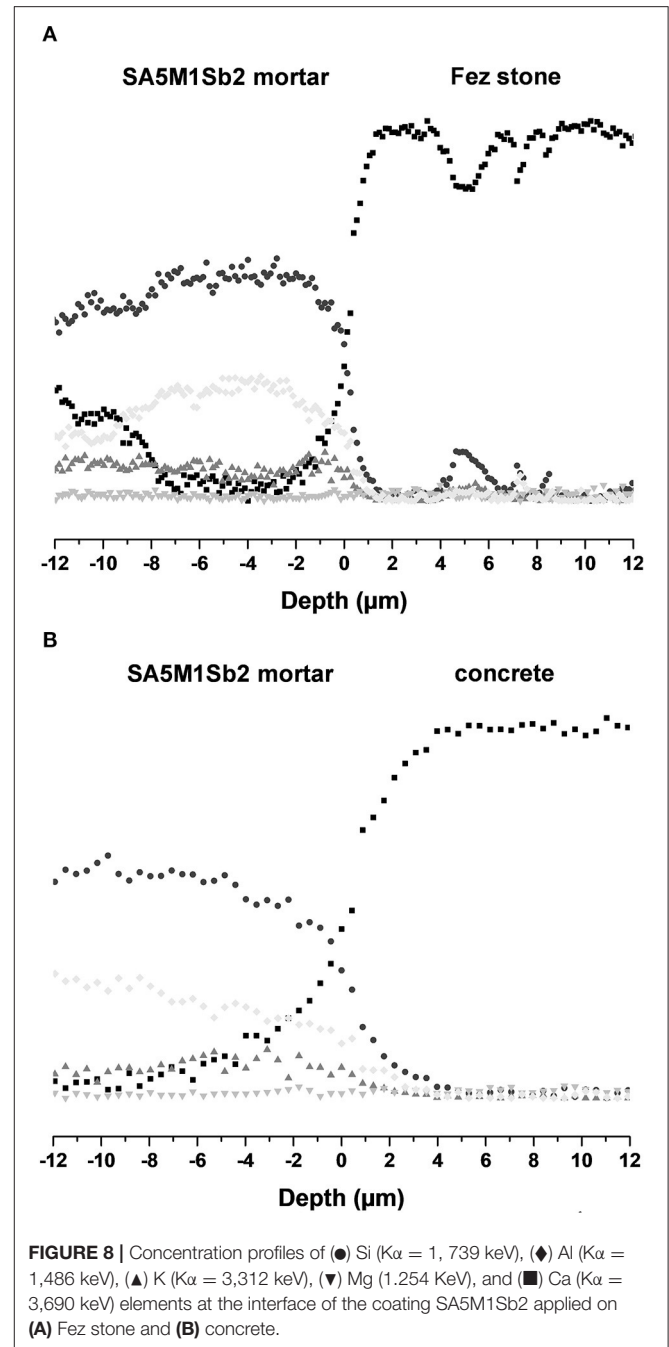
CONCLUSION

The objective of this study was to evaluate the suitability of a geopolymer binder and mortars based on local Moroccan clays and sands as coatings for the restoration of historical monuments in Morocco. For this, on one hand, five substrates (white and blue limestone, plaster, concrete, and Fez stone) were studied. The natural stones (white and blue limestone and Fez stone) were characterized by lower pH value, capillarity and percentage of open porosity, and higher contact angle compared to concrete and plaster. Furthermore, concrete and Fez stone exhibited higher roughness surface values than limestones and plaster. On the other hand, a geopolymer binder based on metakaolin and two geopolymer mortars based on a mixture of metakaolin, two Moroccan clays, and two sands were selected and successfully applied by airbrush on the different substrates with thickness varying between 340 and 650 µm. This thickness was related to coating features such as viscosity, liquid to solid ratio, and granular skeleton in the case of mortar as well as substrate surface roughness.

In order to verify the adhesion and the stability of the different coatings, they were stored in different conditions (different temperatures and relative humidity). It is evidenced that the obtained adhesive strength values decreased especially for the



white and blue limestone with the increase of relative humidity or weathering conditions. However, quite stable adhesive strength values of about 3 MPa were obtained for Fez stone, regardless of the coating formulation, at the different storage conditions which



were sufficient for restoration application. The adhesion between the coating and the different substrates was evidenced by SEM observations and concentration profiles. These results confirm the suitability of coatings based on metakaolin, Moroccan clays, and sands for restoration applications.

DATA AVAILABILITY STATEMENT

The original contributions presented in the study are included in the article/**Supplementary Material**, further inquiries can be directed to the corresponding author/s.

AUTHOR CONTRIBUTIONS

AE: experimental test. RF: Figures. PD: SEM experiments. AG, NI, AZ, and SR: redaction. All authors contributed to the article and approved the submitted version.

REFERENCES

- Apostolopoulou, M., Aggelakopoulou, E., Bakolas, A., and Moropoulou, A. (2018). "Compatible mortars for the sustainable conservation of stone in masonries," in *Advanced Materials for the Conservation of Stone*, eds M. Hosseini and I. Karapanagiotis (Cham: Springer). doi: 10.1007/978-3-319-72260-3_5
- Arnoult, M., Perronnet, M., Autef, A., and Rossignol, S. (2018). How to control the geopolymer setting time with the alkaline silicate solution. *J. Non Cryst. Solids* 495, 59–66. doi: 10.1016/j.jnoncrysol.2018.02.036
- Benharbit, M. (2017). Cement mortar restorations and disorders in the archaeological site of Chellah. *Int. J. Adv. Eng. Res. Sci.* 4, 11–14. doi: 10.22161/ijaers.4.8.2
- Benjeddou, O., Soussi, C., Jedidi, M., and Benali, M. (2017). Experimental and theoretical study of the effect of the particle size of limestone fillers on the rheology of self-compacting concrete. *J. Build. Eng.* 10, 32–41. doi: 10.1016/j.job.2017.02.003
- Bozkurt, T. S., and Yilmaz Demirkale, S. (2020). Investigation and development of sound absorption of plasters prepared with pumice aggregate and natural hydraulic lime binder. *Appl. Acoust.* 170:107521. doi: 10.1016/j.apacoust.2020.107521
- Chiche, A., Pareige, P., and Creton, C. (2000). Role of surface roughness in controlling the adhesion of a soft adhesive on a hard surface. *Comptes Rendus de l'Académie des Sci. Ser. IV Phys.* 1, 1197–1204. doi: 10.1016/S1296-2147(00)01133-1
- Ciantia, M. O., Castellanza, R., and di Prisco, C. (2014). Experimental Study on the water-induced weakening of calcarenites. *Rock Mech. Rock Eng.* 48, 441–461. doi: 10.1007/s00603-014-0603-z
- Dalehaug, A. (2005). *Measurement of Water Retention Properties of Plaster. A Parameter Study of the Influence on Moisture Balance of an External Wall Construction from Variations of This Parameter*. Norwegian Building Research Institute.
- Deshmukh, K., Parsai, R., Anshul, A., Singh, A., Bharadwaj, P., Gupta, R., et al. (2017). Studies on fly ash based geopolymeric material for coating on mild steel by paint brush technique. *Int. J. Adhesion Adhesives* 75, 139–144. doi: 10.1016/j.ijadhadh.2017.03.002
- Dupuy, C., Gharzouni, A., Sobrados, I., Tessier-Doyen, N., Texier-Mandoki, N., Bourbon, X., et al. (2020). Formulation of an alkali-activated grout based on Callovo-Oxfordian argillite for an application in geological radioactive waste disposal. *Constr. Build. Mater.* 232:117170. doi: 10.1016/j.conbuildmat.2019.117170
- Duxson, P., Provis, J. L., Lukey, G. C., and van Deventer, J. S. J. (2006). ³⁹K NMR of free potassium in geopolymers. *Ind. Eng. Chem. Res.* 45, 9208–9210. doi: 10.1021/ie060838g
- El Alami, K., Asbik, M., and Agalit, H. (2020). Identification of natural rocks as storage materials in thermal energy storage (TES) system of concentrated solar power (CSP) plants – a review. *Solar Energy Mater. Solar Cells* 217:110599. doi: 10.1016/j.solmat.2020.110599
- El Khomsi, A., Gharzouni, A., Kandri, N. I., Zerouale, A., and Rossignol, S. (2020). Properties of geopolymer composites from two different Moroccan clays. *Ceram. Modern Technol.* 2, 62–69. doi: 10.29272/cmt.202.0.0001
- Gajanan Kunde, B., and Ganapati Yadav, D. (2016). Green approach in the sol-gel synthesis of defect free unsupported mesoporous alumina films. *Micropor. Mesopor. Mater.* 224, 43–50. doi: 10.1016/j.micromeso.2015.10.045
- Hanzlíček, T., Steinerova, M., Straka, P., Perna, I., Siegl, P., and Švarcova, T. (2009). Reinforcement of the terracotta sculpture by geopolymer composite. *Mater. Design* 30, 3229–3234. doi: 10.1016/j.matdes.2008.12.015

SUPPLEMENTARY MATERIAL

The Supplementary Material for this article can be found online at: <https://www.frontiersin.org/articles/10.3389/fceng.2021.667982/full#supplementary-material>

- ICOMOS (2004). "ICOMOS Charter « Principles for the Analysis, Conservation and Structural Restoration of Architectural Heritage »- 2003," in *International Charters for Conservation and Restoration - Monument and Sites Volume I*, ed ICOMOS (München: Lipp GmbH).
- Jiang, C., Wang, A., Bao, X., Chen, Z., Ni, T., and Wang, Z. (2020). Protective geopolymer coatings containing multi-componential precursors: preparation and basic properties characterization. *Materials* 13:3448. doi: 10.3390/ma13163448
- Kirilovica, I., Vitina, I., and Lindina, L. (2018). Hydration of cement minerals in a hydraulic dolomitic binder. *Key Eng. Mater.* 762, 356–336. doi: 10.4028/www.scientific.net/KEM.762.356
- Loureiro, M. S., Paz, S. P. A. D., Veiga, M. D. R., and Angélica, R. S. (2020). Investigation of historical mortars from Belém do Pará, Northern Brazil. *Constr. Build. Mater.* 233:117284. doi: 10.1016/j.conbuildmat.2019.117284
- Mao, Y., Biasetto, L., and Colombo, P. (2020). Metakaolin-based geopolymer coatings on metals by airbrush spray deposition. *J. Coat. Technol. Res.* 17, 991–1002. doi: 10.1007/s11998-019-00310-6
- Moropoulou, A., Aggelakopoulou, E. E., and Bakolas, A. (2006). "Earthquakes and monuments—the role of materials in the earthquake protection of monuments," in *5th International Conference on Structural Analysis of Historical Constructions, Vol. 3*, eds P. B. Lourenço, P. Roca, C. Modena, and S. Agrawal (New Delhi), 1625–1631.
- Moropoulou, A., Bakolas, A., Moundoulas, P., and Aggelakopoulou, E. (2005). "Reverse engineering: a proper methodology for compatible restoration mortars," in *Proceedings of the Workshop Repair Mortars for Historic Masonry, TC RMH*. (Delft: RILEM), 25–28.
- Moropoulou, A., Bakolas, A., Moundoulas, P., and Cakmak, A. S. (1998). Compatible restoration mortars, preparation and evaluation for Hagia Sophia earthquake protection. *PACT* 56, 79–118.
- Moutinho, H. R., Jiang, C. S., To, B., Perkins, C., Muller, M., and Al-Jassim, M. M. L. (2017). Simpson Adhesion mechanisms on solar glass: effects of relative humidity, surface roughness, and particle shape and size. *Solar Energy Mater. Solar Cells* 172, 145–153. doi: 10.1016/j.solmat.2017.07.026
- Najafi Kani, B., Allahverdi, A., and Provis, J. L. (2012). Efflorescence control in geopolymer binders based on natural Pozzolan. *Cement Concrete Compos.* 34, 25–33. doi: 10.1016/j.cemconcomp.2011.07.007
- Nogami, L., Paraguassú, A. B., and Rodrigues, J. E. (2015). Adhesive mortars for stone plate bonding. *Bull. Eng. Geol. Environ.* 74, 1489–1497. doi: 10.1007/s10064-014-0708-3
- Occhipinti, R., Strosio, A., Finocchiaro, C., Fugazzotto, M., Leonelli, C., José Lo Faro, M., et al. (2020). Alkali activated materials using pumice from the Aeolian Islands (Sicily, Italy) and their potentiality for cultural heritage applications: preliminary study. *Constr. Build. Mater.* 259:120391. doi: 10.1016/j.conbuildmat.2020.120391
- Pareek, S., Kashima, H., Maruyama, I., and Araki, Y. (2018). Adhesion characteristics of geopolymer mortar to concrete and rebars. *MATEC Web Conf.* 258:5801012. doi: 10.1051/mateconf/201925801012
- Pierre, A. C. (1992). *Introduction aux procédés sol – gel*. Collection FORCE RAM, Editions SEPTIMA (Paris).
- Piovesan, R., Maritan, L., Meneghin, G., Previato, C., Baklouti, S., Sassi, R., et al. (2019). Stones of the façade of the Sarno Baths, Pompeii: a mindful construction choice. *J. Cult. Herit.* 40, 255–264. doi: 10.1016/j.culher.2019.04.010
- Randazzo, L., Paladini, G., Venuti, V., Crupi, V., Ott, F. C., Montana, G., et al. (2020). Pore structure and water transfer in Pietra d'Aspra Limestone: a neutronographic study. *Appl. Sci.* 10:6745. doi: 10.3390/app10196745
- Rescic, S., Plescia, P., Cossari, P., Tempesta, E., Capitani, D., Proietti, N., et al. (2011). Mechano- chemical activation: an ecological safety process in the

- production of materials to stone conservation. *Proc. Eng.* 21, 1061–1071. doi: 10.1016/j.proeng.2011.11.2112
- Sanjay Latthe, S., Rajaram Sutar, S., Vishnu Kodag, S., Bhosale, A. K., Madhan Kumar, A., Kumar Sadasivuni, K., et al. (2019). Self – cleaning superhydrophobic coatings: potential industrial applications. *Progr. Organ. Coat.* 128, 52–58. doi: 10.1016/j.porgcoat.2018.12.008
- Schueremans, L., Cizer, Ö., Janssens, E., Serré, G., and Balen, K. V. (2011). Characterization of repair mortars for the assessment of their compatibility in restoration projects: research and practice. *Constr. Build. Mater.* 25, 4338–4350. doi: 10.1016/j.conbuildmat.2011.01.008
- Secco, M., Previato, C., Addis, A., Zago, G., Kamsteeg, A., Dilaria, S., et al. (2019). Mineralogical clustering of the structural mortars from the Sarno Baths, Pompeii: a tool to interpret construction techniques and relative chronologies. *J. Cult. Herit.* 40, 265–273. doi: 10.1016/j.culher.2019.04.016
- Sharma, K. V., Vardhan Sharma, K., Nicolinia, J. V., de Araujo, O. M. O., Strakac, R., Ferraza, H. C., et al. (2018). Laser-induced wettability alteration in limestone rocks. *Mater. Today Commun.* 17, 332–340. doi: 10.1016/j.mtcomm.2018.09.012
- Skvara, F., Kopecky, L., Nimeek, J., and Bittnar, Z. (2006). Microstructure of geopolymer materials based on fly ash. *Ceram Silik* 50, 208–215.
- Temuujin, J., Minjigmaa, A., Rickard, W., Lee, M., Williams, I., and van Riessen, A. (2010). Fly ash based geopolymer thin coatings on metal substrates and its thermal evaluation. *J. Hazardous Mater.* 180, 748–752. doi: 10.1016/j.jhazmat.2010.04.121
- Ventola, L., Vendrell, M., Giraldez, P., and Merino, L. (2011). Traditional organic additives improve lime mortars: new old materials for restoration and building natural stone fabric. *Constr. Build. Mater.* 25, 3313–3318. doi: 10.1016/j.conbuildmat.2011.03.020
- Waples, D. W., and Waples, J. S. (2004). A review and evaluation of specific heat capacities of rocks, minerals, and subsurface fluids. Part 1: minerals and nonporous rocks. *Nat. Resour. Res.* 13, 97–122. doi: 10.1023/B:NARR.0000032647.41046.e7
- Zhang, Z., Yao, X., and Zhu, H. (2010). Potential application of geopolymers as protection coatings for marine concrete 1. Basic properties. *Appl. Clay Sci.* 49, 1–6. doi: 10.1016/j.clay.2010.01.014

Conflict of Interest: The authors declare that the research was conducted in the absence of any commercial or financial relationships that could be construed as a potential conflict of interest.

Copyright © 2021 El Khomsi, Gharzouni, Farges, Duport, Idrissi Kandri, Zerouale and Rossignol. This is an open-access article distributed under the terms of the Creative Commons Attribution License (CC BY). The use, distribution or reproduction in other forums is permitted, provided the original author(s) and the copyright owner(s) are credited and that the original publication in this journal is cited, in accordance with accepted academic practice. No use, distribution or reproduction is permitted which does not comply with these terms.